

# Usability Evaluation of Optimized Digital Elevation Model Derived from Unmanned Aerial Vehicle Light Detection and Ranging Data for Settlement Estimation of Soft Ground

Jae-Cheol Lee,<sup>1</sup> Dong-Ha Lee,<sup>1\*</sup> and Jae-Bin Lee<sup>2\*\*</sup>

<sup>1</sup>Department of Integrated Energy and Infra System, Kangwon National University,  
1 Kangwondaehak-gil, Chuncheon-si, Gangwon-do 24341, Republic of Korea

<sup>2</sup>Department of Architectural, Civil and Environmental Engineering, Mokpo National University,  
Muan, Jeonnam 58554, Republic of Korea

(Received August 22, 2024; accepted September 12, 2024)

**Keywords:** digital elevation model, settlement estimation, soft ground, UAV LiDAR, utility

Currently, the settlement of soft ground is measured using instruments operated by on-site workers. However, this method is expensive and inefficient in terms of data consistency, cost-effectiveness, and utility. On the other hand, surveying using unmanned aerial vehicle (UAV) light detection and ranging (LiDAR) is used in various fields. However, studies on its utility in soft ground are insufficient. Therefore, in this study, we examined the optimal method for creating digital elevation models (DEMs) for estimating the settlement of soft ground using UAV LiDAR survey data. This method involved selecting a coastal construction site as the study area and acquiring data through UAV LiDAR surveying. The acquired data were used to create DEMs through preprocessing and postprocessing. Settlement measurements obtained from on-site instruments and settlement estimates derived from DEMs created using various interpolation methods and grid sizes were compared and analyzed. Additionally, the utility of the created time-series DEMs in the settlement estimation of soft ground was evaluated. We proposed the optimal method for creating DEMs for estimating the settlement of soft ground and suggested methods to utilize the proposed time-series DEMs. Our research results show that the use of UAV LiDAR survey data can lead to the economical and efficient settlement estimation of soft ground.

## 1. Introduction

South Korea is a peninsula surrounded on three sides by the sea. Owing to these geographical characteristics, construction projects for expanding social overhead capital facilities such as airports, ports, maritime logistics bases, and marine leisure facilities have steadily increased to enhance efficient land use and promote balanced regional development.<sup>(1)</sup> Most of these projects are conducted by creating land through the deposition of dredged materials obtained from nearby waters after constructing breakwaters in coastal areas, inevitably leading to the formation

---

\*Corresponding author: e-mail: [geodesy@kangwon.ac.kr](mailto:geodesy@kangwon.ac.kr)

\*\*Corresponding author: e-mail: [lee2009@mnu.ac.kr](mailto:lee2009@mnu.ac.kr)

<https://doi.org/10.18494/SAM5313>

of soft ground because of the nature of the fill material. Such soft ground causes various engineering problems, including stability issues because of the low shear strength of the fill material, settlement problems arising from decreased volume as pore water pressure decreases under applied loads, and liquefaction issues due to increased excess pore water pressure from rapid reductions in ground strength and volume during dynamic loading,<sup>(2)</sup> necessitating systematic settlement measurements in advance.

Although the settlement measurement of soft ground is conducted using data from on-site instruments, this method is inefficient because of difficulties in observation caused by site conditions and weather changes and the inability to obtain data in areas without instruments.<sup>(3)</sup> Moreover, this method has economic limitations, such as errors attributable to the operator's skill level and instrument displacement, as well as reduced measurement frequency due to increased labor costs for transport and installation.<sup>(4,5)</sup>

On the other hand, advancements in digital technology are being integrated and utilized in various construction industrial sectors alongside traditional construction technologies. Unmanned aerial vehicle (UAV) light detection and ranging (LiDAR) surveying, with its combined characteristics of excellent consistency, accessibility, and flexibility in monitoring and surveying with high accuracy and precision, along with high-resolution 3D mapping, is significantly more economical and efficient than traditional surveying methods and is used in various construction industry fields.<sup>(6)</sup>

Studies on the use of UAV LiDAR in the construction industry have been reviewed, which mainly focused on evaluating the stability of earthwork slopes, road construction, and maintenance, calculating cut and fill volumes during earthworks, and collecting terrain information for open-pit mines.<sup>(7-10)</sup> Recently, studies on settlement estimation and identifying abnormal settlement phenomena in soft ground<sup>(11,12)</sup> have been reported. However, studies on the use of digital elevation models (DEMs) created with UAV LiDAR survey data for the settlement estimation of soft ground are still scarce.

Therefore, in this study, we selected a construction site undergoing land reclamation in a coastal area as the study area and acquired data through UAV LiDAR surveying. The acquired data were processed to obtain useful 3D spatial information, and a DEM was created using various interpolation methods and grid sizes. Settlement estimates from 12 selected settlement measurement instruments in the study area and those derived from DEMs created using UAV LiDAR survey data were compared and analyzed to evaluate the optimal method for creating DEMs for the settlement estimation of soft ground. Additionally, the utility of the optimized time-series DEMs for settlement estimation in soft ground was assessed. On the basis of the obtained results, we optimized DEMs created with UAV LiDAR survey data and evaluated their utility, which we found to be a more economical and efficient alternative to the traditional on-site instrument methods currently used for the settlement estimation of soft ground.

## 2. Analysis of Current Settlement Measurements of Soft Ground

After selecting a coastal construction site undergoing land reclamation as the study area, the current status of settlement measurements at the site was investigated, and UAV LiDAR

surveying was conducted to acquire data. The acquired data were processed to obtain useful 3D spatial information, and a DEM was created using various interpolation methods and grid sizes. By comparing and analyzing settlement estimates from 12 selected measurement instruments and those derived from DEMs created using UAV LiDAR survey data, we analyzed optimal DEM creation methods for the settlement estimation of soft ground and proposed their utility.

## 2.1 Study area

The study area was selected considering a site undergoing land reclamation through dredged material deposition in coastal waters, as shown in Fig. 1. The selected study area is the “Busan New Port West Container Terminal Phase 2-6 Construction” site located in the waters east of Yeondo and Songdo, Ongcheon-dong, Jinhae City, Gyeongsangnam-do. The project involved the construction of two berths (700 m) for a container terminal and improving the soft ground in the dredging and reclamation area to create the site. The soft ground area is approximately 391,535 m<sup>2</sup>, and 58 surface settlement plates are used to measure settlement to manage the consolidation and settlement of the soft ground.

## 2.2 Status and results of surface settlement plate measurements

To optimize the DEM through the comparison and analysis of settlement estimates using surface settlement plates installed in the study area and those derived from UAV LiDAR surveying, 12 plates were selected considering the area and instrument distribution at the site (Fig. 2).

For comparison and analysis with DEM estimates, among the results from the 12 selected measurements, the data obtained on May 26, 2021, corresponding to the UAV LiDAR observation date, are presented in Table 1.

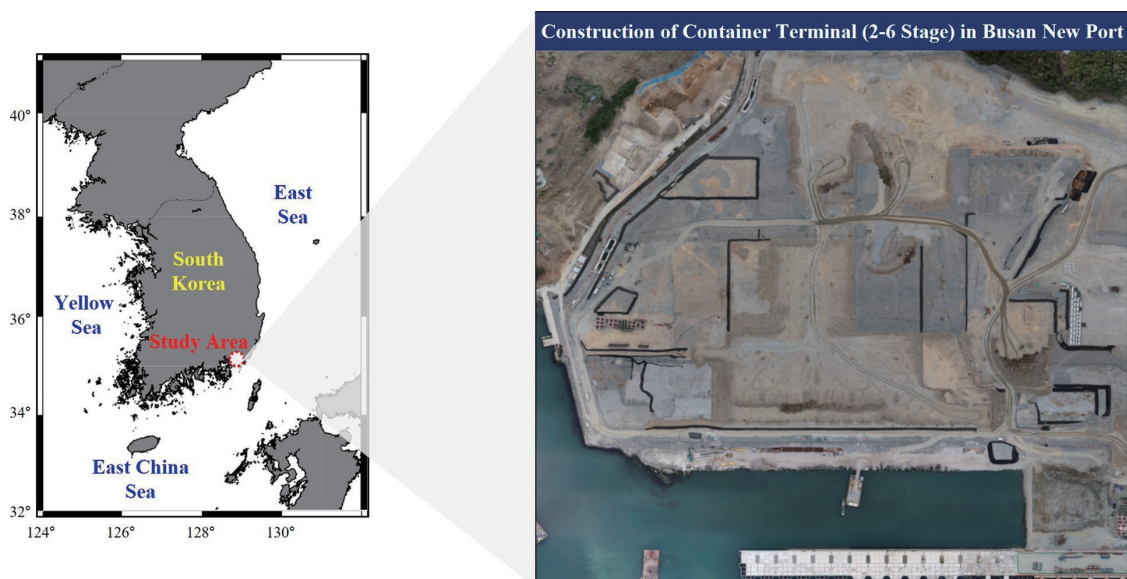


Fig. 1. (Color online) Study area.

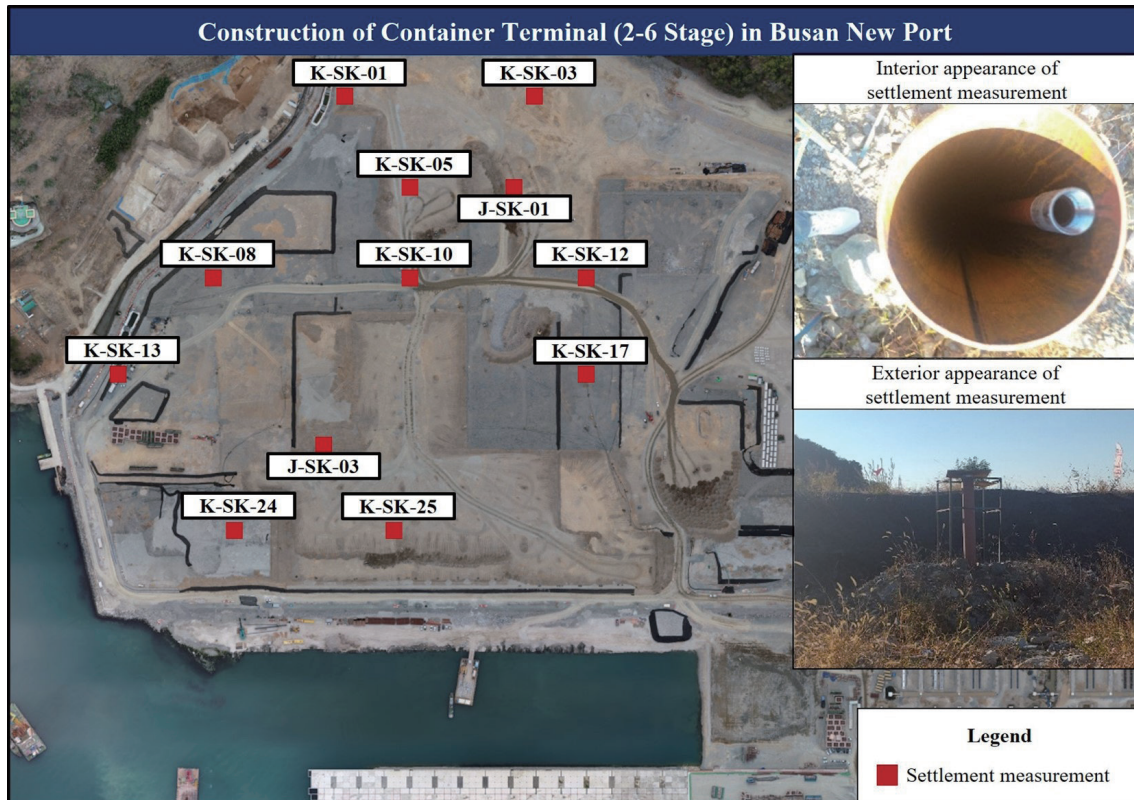


Fig. 2. (Color online) Distribution status of settlement measurements in study area.

Table 1  
Settlement measurement instrument locations and heights.

No.	Measuring point	Transverse Mercator coordinates		Orthometric height (m)
		X	Y	
1	J-SK-01	274761.0010	178849.2670	8.819
2	J-SK-03	274551.0019	179149.2670	5.069
3	K-SK-01	274586.1306	178749.2670	9.880
4	K-SK-03	274786.1306	178749.2670	9.356
5	K-SK-05	274651.0019	178849.2670	9.924
6	K-SK-08	274451.0019	178949.2670	8.632
7	K-SK-10	274651.0019	178949.2670	8.762
8	K-SK-12	274851.0019	178949.2670	8.010
9	K-SK-13	274351.0019	179049.2670	8.716
10	K-SK-17	274851.0019	179049.2670	7.416
11	K-SK-24	274476.9003	179229.3229	6.845
12	K-SK-25	274639.8040	179213.6826	6.686

### 3. UAV LiDAR Surveying

To create the DEM from UAV LiDAR survey data, observations were conducted in the study area. The raw data obtained from the survey were converted into meaningful 3D spatial information through preprocessing. The preprocessing involved calculating 3D spatial



coordinates for the study area using the global navigation satellite system (GNSS) and inertial navigation system (INS) data, LiDAR data, and ground GNSS base station data, integrating hardware characteristics of the UAV LiDAR system, distances between installed sensors, and the calibration information of the UAV (Fig. 3).

### 3.1 UAV LiDAR survey overview

The UAV LiDAR survey was conducted on May 26, 2021. The study area, a site with soft ground created through dredged material reclamation, had no obstructions in the flight path. The flight path was planned and executed considering the weather, GNSS satellite configurations, UAV speed and direction, and the distance to ground reference points, as shown in Fig. 4. Additionally, the LiDAR equipment used in the study was Velodyne's 3D scanner VLP

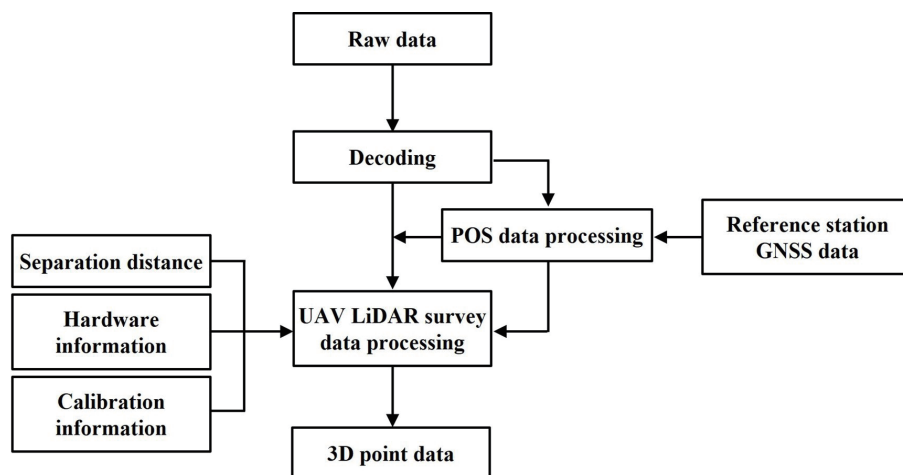


Fig. 3. UAV LiDAR survey data preprocessing flow.

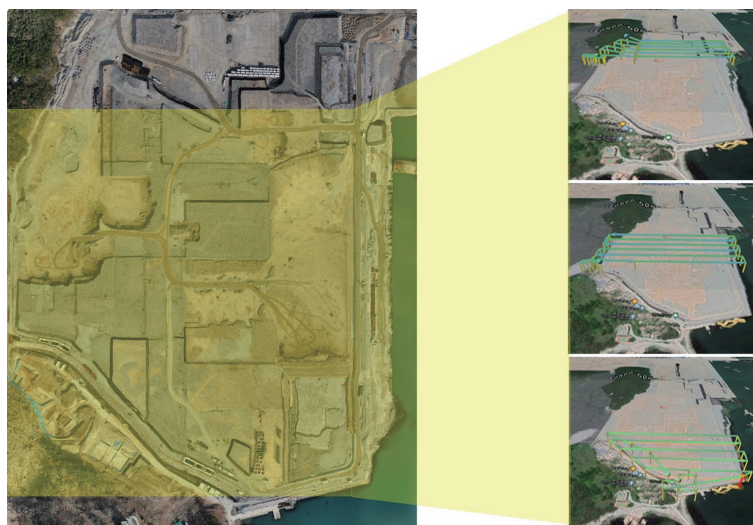


Fig. 4. (Color online) UAV LiDAR flight path.

(Velodyne LiDAR PUCK)-16, and the data processing software used was TerraSolid’s TerraScan (Table 2).

### 3.2 UAV LiDAR data processing

The processing of GNSS/INS data must precede that of the raw data obtained by UAV LiDAR observation, as shown in Fig. 5.

Precise positional information was obtained through DGNSS processing, which uses the location information received by the UAV and GNSS base station. The GNSS/INS data used for UAV LiDAR data processing include the position and attitude information of the UAV. After GNSS/INS processing, the quality of observation data was evaluated on the basis of the number of visible satellites and the dilution of precision (DOP) values on each observation date. No

Table 2  
Measurement equipment and software.

	VLP-16		TerraScan
Model name	Velodyne LiDAR Puck LITE	Data Input	Compatible with various LiDAR and imaging data formats.
Range	Maximum Range: Up to 100 m		
Data Output	Point Clouds: Up to 300000 points per second	Data Processing	Point cloud classification and segmentation Advanced filtering and cleaning tools Georeferencing and coordinate transformation
	Data Rate: 600000 points per second (dual return)		
Accuracy	Range: ±3 cm (typical) Azimuth: 0.1° (typical)		

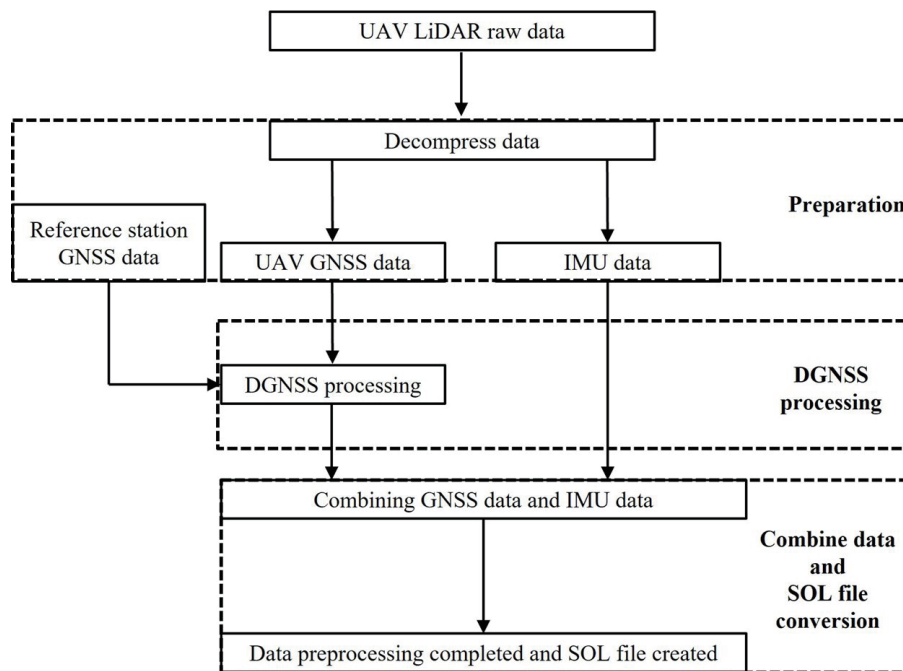


Fig. 5. GNSS/INS data processing flow.

signal interruptions occurred during the UAV flight, the separation error during UAV cross flights was within 10 cm, the DOP value was 3 or less, and at least six visible GNSS satellites were used, ensuring the accuracy and reliability of the survey data.

The acquired GNSS data were linked and adjusted with data from GNSS continuous observation stations to accurately produce World Geodetic System coordinates, completing the preprocessing of UAV LiDAR data for the study area (Figs. 6 and 7).

#### 4. DEM Creation and Optimization Analysis

To optimize the DEM for the settlement estimation of soft ground, the high-precision 3D spatial information obtained through the preprocessing of UAV LiDAR data must be

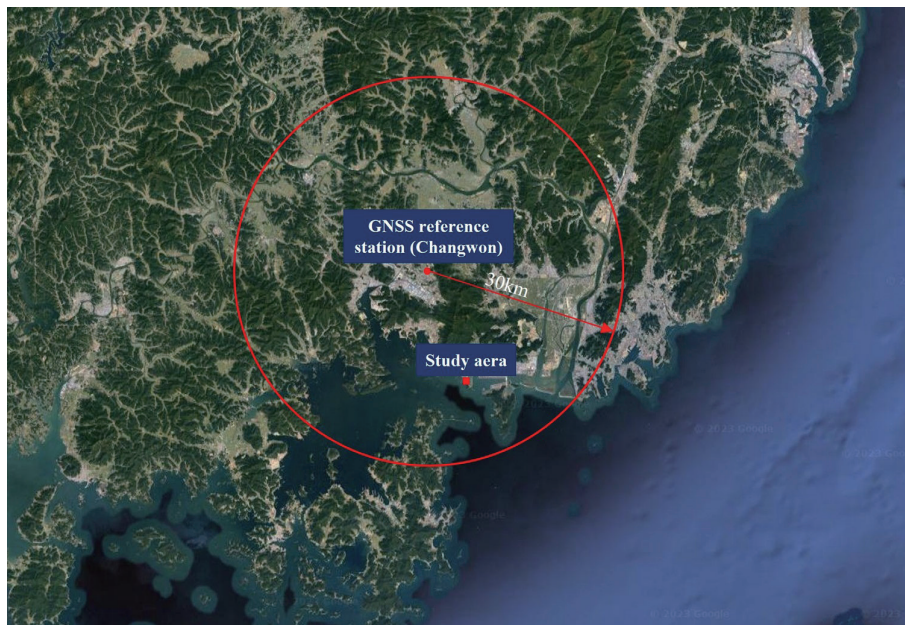


Fig. 6. (Color online) GNSS reference station location and baseline distance.

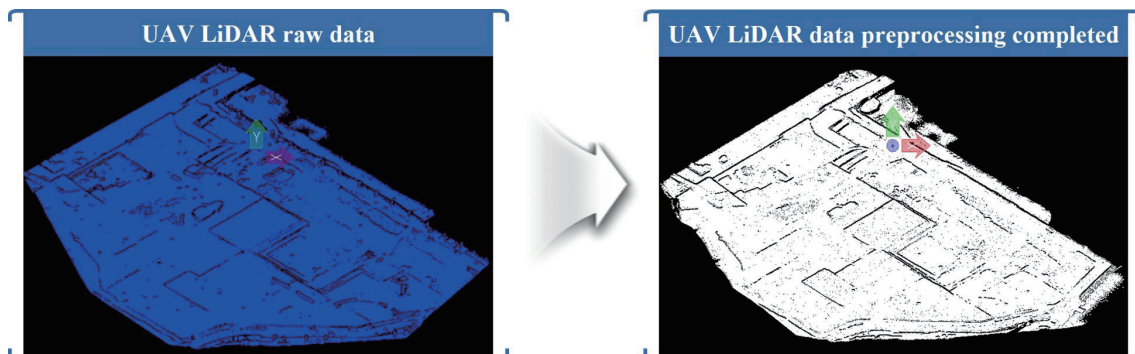


Fig. 7. (Color online) UAV LiDAR data preprocessing result.

postprocessed, including data refinement and classification. In the postprocessing stage, a series of steps such as orthometric height conversion and data classification are performed to develop the final DEM (Fig. 8).

Orthometric height conversion involves converting the ellipsoidal height data acquired from UAV LiDAR surveying to orthometric height data by applying a geoid correction. In this study, we used the national geoid model (KNGeoid18) provided by the National Geographic Information Institute, known to have a precision of  $\pm 2.33$  cm.<sup>(13)</sup> Upon examining the converted orthometric height data, the conversion range for the study area was confirmed to be 28.19 m to 28.22 m (Fig. 9).

In UAV LiDAR surveying, the height from the ground surface is calculated from the distance proportional to the time required for the signal to reflect off the terrain, structures, or vegetation. Data classification based on reflection intensity and echo is also performed, and the extracted data are categorized by layer. Therefore, a terrain classification step was conducted to separate layers such as obstructions and trees in the study area that were not related to the research objectives (Fig. 10).

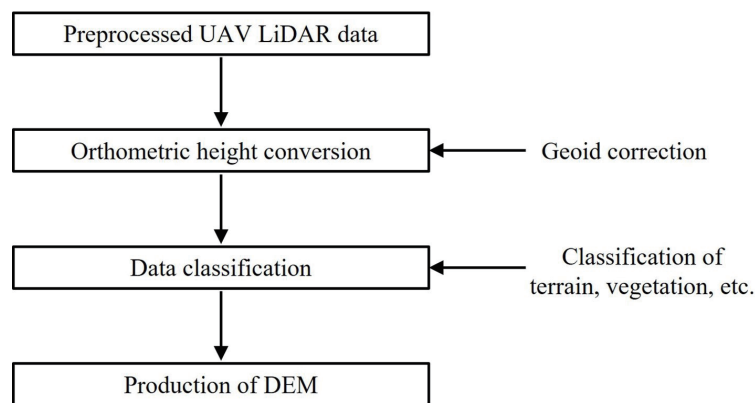


Fig. 8. DEM production process.

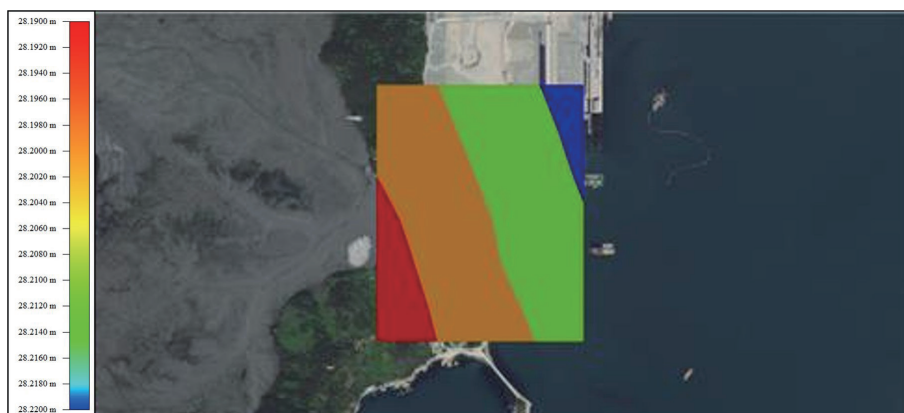


Fig. 9. (Color online) Orthometric height conversion using KNGeoid18.



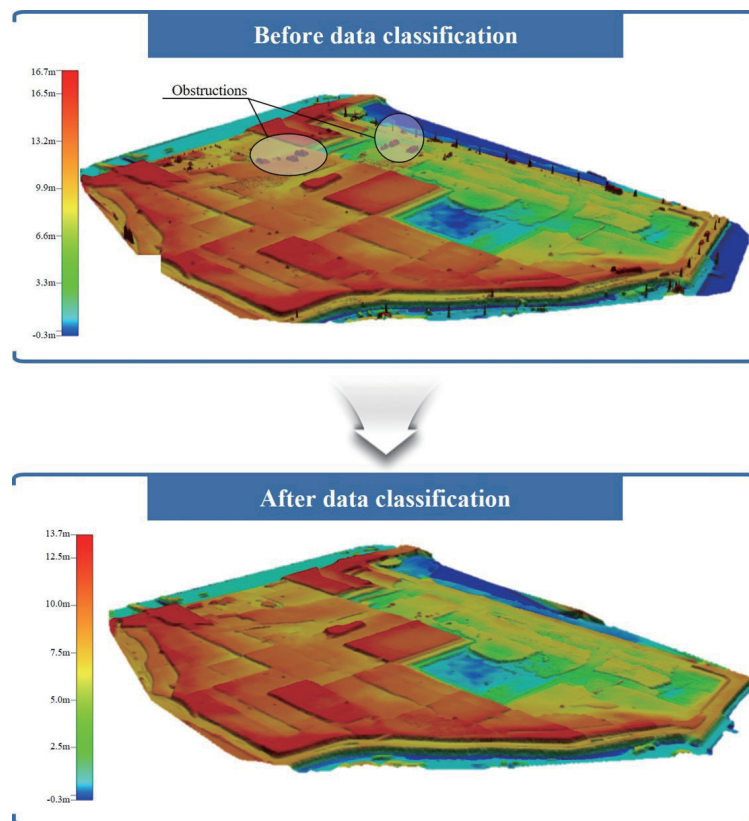


Fig. 10. (Color online) Data classification.

#### 4.1 Determination of optimal interpolation method

Interpolation refers to estimating the elevation values of unmeasured terrain by optimally estimating continuous functions from given data, and various interpolation methods are applied in DEM production. The choice of an interpolation method can vary depending on the characteristics and purpose of DEM production. Factors to consider when applying interpolation methods include data density, distribution, and noise level, and the most appropriate method should be used on the basis of these data characteristics. Additionally, when a smooth representation of surfaces is required for terrain analysis, methods such as spline interpolation or Kriging may be suitable, and appropriate interpolation methods can be applied depending on the intended use.

To explore optimization strategies for DEMs for the settlement estimation of soft ground, we employed commonly used interpolation methods such as Kriging, triangulated irregular network (TIN), and natural neighbor interpolation (NNI) (Fig. 11).

After applying Kriging, TIN, and NNI interpolation methods to produce DEMs for each observation date, orthometric heights at the same locations as the field instruments (surface settlement plates) were calculated (Table 3). The optimal interpolation method was determined by comparing and analyzing the orthometric heights derived from DEMs with those measured using the surface settlement plates in the study area (Table 4).

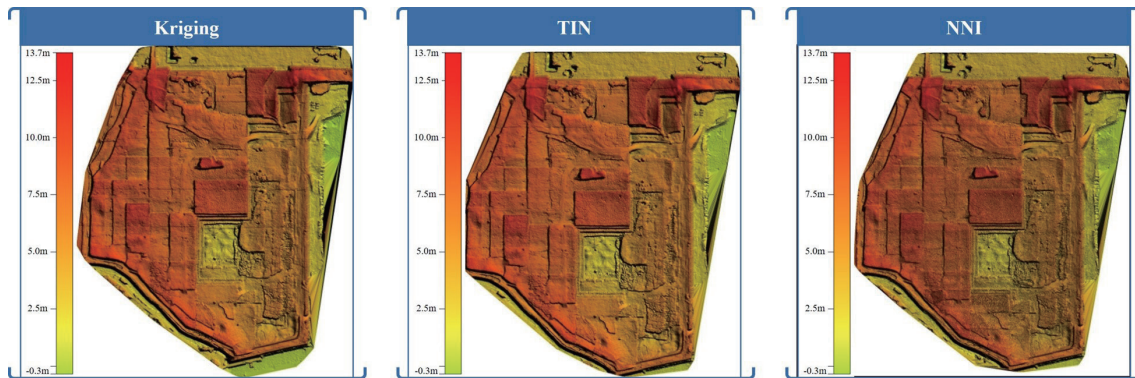


Fig. 11. (Color online) Production of DEM by interpolation method.

Table 3  
Orthometric height of DEM produced by each interpolation method.

No.	Measurement point	Orthometric height of DEM (m)		
		Kriging	TIN	NNI
1	J-SK-01	8.480	8.390	8.390
2	J-SK-03	5.170	5.190	5.130
3	K-SK-01	9.600	9.500	9.460
4	K-SK-03	9.160	9.140	9.050
5	K-SK-05	9.500	9.450	9.390
6	K-SK-08	8.070	7.990	7.960
7	K-SK-10	8.700	8.570	8.550
8	K-SK-12	7.950	7.690	7.950
9	K-SK-13	8.770	8.770	8.730
10	K-SK-17	7.010	6.990	6.920
11	K-SK-24	5.950	5.910	5.880
12	K-SK-25	6.490	6.400	6.370

Table 4  
Comparison of orthometric height between settlement measurements and DEM calculation values.

No.	Measurement point	Deviation (m)		
		Kriging	TIN	NNI
1	J-SK-01	0.339	0.429	0.429
2	J-SK-03	-0.101	-0.121	-0.061
3	K-SK-01	0.280	0.380	0.420
4	K-SK-03	0.196	0.216	0.306
5	K-SK-05	0.424	0.474	0.534
6	K-SK-08	0.562	0.642	0.672
7	K-SK-10	0.062	0.192	0.212
8	K-SK-12	0.060	0.320	0.060
9	K-SK-13	-0.054	-0.054	-0.014
10	K-SK-17	0.406	0.426	0.496
11	K-SK-24	0.895	0.935	0.965
12	K-SK-25	0.196	0.286	0.316
	Minimum	-0.101	-0.121	-0.061
	Maximum	0.895	0.935	0.965
	Average	0.272	0.344	0.361
	RMSE	±0.280	±0.284	±0.295

The comparison and analysis of settlement estimation results from DEMs created using different interpolation methods and results from settlement measurement instruments revealed that the Kriging interpolation method had the smallest deviation values, with a minimum deviation of  $-0.101$  m, a maximum deviation of  $0.895$  m, an average deviation of  $0.272$  m, and a root mean square error (*RMSE*) of  $\pm 0.280$ , which are most similar to the instrument values. The NNI interpolation method showed the largest difference from the instrument values, with a minimum deviation of  $0.061$  m, a maximum deviation of  $0.965$  m, an average deviation of  $0.361$  m, and an *RMSE* of  $\pm 0.295$  m.

#### 4.2 Determination of optimal grid size

The determination of the optimal interpolation method showed that the Kriging method results were most similar to the surface settlement plate measurement results. Therefore, to determine the optimal grid size, the observation data from May 26, 2021, were used, and the Kriging method was applied. The grid sizes were set to 0.2, 0.5, 1.0, 1.5, and 2.0 m during DEM production to calculate the orthometric height at the same locations as the field instruments (surface settlement plates) (Table 5).

The optimal grid size was determined by comparing and analyzing the orthometric height results from Table 5 with the orthometric heights measured using the surface settlement plates in the study area (Table 6).

As shown in Table 6, as the grid size decreases, the orthometric height approximate those of the settlement measurement instruments. The 2.0 m grid size exhibited a slightly larger difference than the 1.5 m grid size because the 2.0 m grid size could not accurately reproduce the locations of the settlement measurement instruments. A grid size of 2.0 m or greater was unsuitable for this study. Considering the time required and data volume for DEM production, a grid size of 0.2 m was deemed inappropriate in terms of utility. Therefore, for DEM optimization for the settlement estimation of soft ground, a grid size ranging from 0.5 to 1.0 m was most appropriate. In this study, a grid size of 0.5 m was most suitable, considering the data volume and production time of DEMs.

Table 5  
Orthometric height according to the grid size of the DEM.

No.	Measuring point	Kriging (m)				
		0.2	0.5	1.0	1.5	2.0
1	J-SK-01	8.480	8.480	8.480	8.520	8.770
2	J-SK-03	5.160	5.170	5.170	5.290	5.350
3	K-SK-01	9.710	9.720	9.600	9.550	9.550
4	K-SK-03	9.160	9.160	9.160	9.210	9.230
5	K-SK-05	9.550	9.500	9.500	9.430	9.100
6	K-SK-08	8.340	8.240	8.070	8.570	8.570
7	K-SK-10	8.690	8.690	8.700	8.700	8.750
8	K-SK-12	7.910	7.940	7.950	7.960	8.230
9	K-SK-13	8.760	8.760	8.770	8.950	8.980
10	K-SK-17	6.920	7.000	7.010	7.010	7.010
11	K-SK-24	5.970	5.950	5.950	5.880	5.900
12	K-SK-25	6.420	6.470	6.490	6.630	6.630

Table 6  
Comparison of orthometric height between settlement measurements and DEM calculation values.

No.	Measurement point	Deviation (m)				
		0.2	0.5	1.0	1.5	2.0
1	J-SK-01	0.339	0.339	0.339	0.299	0.049
2	J-SK-03	-0.091	-0.101	-0.101	-0.221	-0.281
3	K-SK-01	0.170	0.160	0.280	0.330	0.330
4	K-SK-03	0.196	0.196	0.196	0.146	0.126
5	K-SK-05	0.374	0.424	0.424	0.494	0.824
6	K-SK-08	0.292	0.392	0.562	0.062	0.062
7	K-SK-10	0.072	0.072	0.062	0.062	0.012
8	K-SK-12	0.100	0.070	0.060	0.050	-0.220
9	K-SK-13	-0.044	-0.044	-0.054	-0.234	-0.264
10	K-SK-17	0.496	0.416	0.406	0.406	0.406
11	K-SK-24	0.875	0.895	0.895	0.965	0.945
12	K-SK-25	0.266	0.216	0.196	0.056	0.056
	Minimum	-0.091	-0.101	-0.101	-0.234	-0.281
	Maximum	0.875	0.895	0.895	0.965	0.945
	Average	0.254	0.253	0.272	0.201	0.170
	<i>RMSE</i>	±0.260	±0.268	±0.280	±0.329	±0.395

## 5. Utility Evaluation

The utility of DEMs created using UAV LiDAR surveying lies in addressing the limitations of point-specific data provided by instruments installed on soft ground. It enables optimal maintenance and planning by creating time-series DEMs to monitor quantitative changes in areas without instruments, analyze changes in soft ground, identify potential risk areas, and develop response strategies. Additionally, it enables rapid and highly accurate data acquisition, including the average, maximum, and minimum settlement across the entire soft ground, even in areas without instruments.

To evaluate the utility of UAV LiDAR, time-series DEMs were developed using UAV LiDAR survey data for the periods from May 26, 2021 to June 9, 2021 (14 days of soft ground settlement), May 26, 2021 to June 23, 2021 (28 days of soft ground settlement), and May 26, 2021 to July 16, 2021 (51 days of soft ground settlement), to analyze the settlement status across the entire soft ground (Fig. 12).

The DEM for 14 days of settlement showed a minimum settlement of -1.310 m, a maximum settlement of 3.440 m, an average settlement of 0.015 m, and an *RMSE* of 0.157 m for the entire soft ground. The DEM for 28 days showed a minimum settlement of -2.220 m, a maximum settlement of 3.800 m, an average settlement of 0.127 m, and an *RMSE* of 0.291 m. The DEM for 51 days showed a minimum settlement of -3.030 m, a maximum settlement of 6.250 m, an average settlement of 0.283 m, and an *RMSE* of 0.615 m (Table 7).

This confirms the capability of DEM to address the limitations of field instruments that only provide local observation results for each point, enabling time-series change analysis and monitoring through a comprehensive quantitative database for the entire soft ground area.



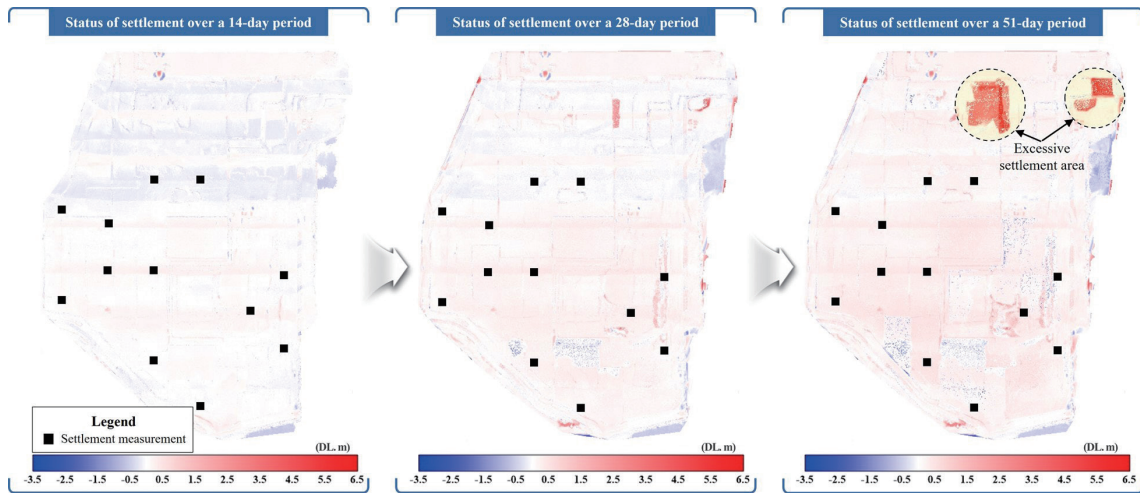


Fig. 12. (Color online) Time-series settlement variation status for the entire soft ground area.

Table 7  
Time-series settlement analysis of the entire soft ground area.

Item	Time-series settlement (m)		
	14 days	28 days	51 days
Minimum	-1.310	-2.220	-3.030
Maximum	3.440	3.800	6.250
Average	0.015	0.127	0.283
<i>RMSE</i>	0.157	0.291	0.615

## 6. Conclusion

In this study, we analyzed the status of settlement measurement using field instruments at the selected study site where land was created by dredged material reclamation in coastal areas to optimize and evaluate the utility of DEMs using UAV LiDAR survey data for the settlement estimation of soft ground. High-precision 3D spatial information was obtained through the preprocessing and postprocessing of UAV LiDAR survey data, and the optimal interpolation method was determined by applying the most widely used Kriging, TIN, and NNI interpolation methods. The optimal grid size was determined by applying different grid sizes for DEM optimization. The main results can be summarized as follows:

1. To determine the optimal interpolation method, the settlement estimation results from DEMs using Kriging, TIN, and NNI interpolation methods and the results from settlement measurement instruments were compared and analyzed. The Kriging interpolation method showed the smallest deviation, with a minimum deviation of 0.101 m, a maximum deviation of 0.895 m, an average deviation of 0.272 m, and an *RMSE* of  $\pm 0.280$ , which are most similar to the instrument values. The NNI interpolation method showed the greatest difference, with a minimum deviation of 0.061 m, a maximum deviation of 0.965 m, an average deviation of 0.361 m, and an *RMSE* of  $\pm 0.295$  m, confirming that Kriging is the most suitable interpolation method.

2. To determine the optimal grid size, the results for grid sizes of 0.2, 0.5, 1.0, 1.5, and 2.0 m were compared with the measurement values of 12 settlement measurement points. The results indicated that grid sizes of 2.0 m or greater were unsuitable for this study, and that compared with a grid size of 0.5 m, a grid size of 0.2 m was inappropriate because of its excessive data volume and time required for DEM production. Therefore, the most appropriate grid size was between 0.5 and 1.0 m, with 0.5 m being identified as the most suitable in this study.
3. To evaluate the utility of DEMs, time-series DEMs were created using UAV LiDAR survey data for the periods from May 26, 2021 to June 9, 2021 (14 days of soft ground settlement), May 26, 2021 to June 23, 2021 (28 days of soft ground settlement), and May 26, 2021 to July 16, 2021 (51 days of soft ground settlement) to analyze the settlement status across the entire soft ground. This enabled the analysis of an overall trend of the settlement through quantitative data acquisition in areas without field instruments, potentially addressing the limitations of localized observations provided by field instruments. This facilitates the identification of changes in areas without field instruments and the development of optimal maintenance plans through rapid response strategies for anticipated problem areas. Our research results show that the use of UAV LiDAR survey data can lead to the economical and efficient settlement estimation of soft ground.

From the results of this study, optimal methods of creating DEMs and their utility for the settlement estimation of soft ground were explored. As UAV LiDAR survey technology is rapidly advancing, continuous follow-up research is necessary to derive more accurate and economical DEM construction methods in the future.

### Acknowledgments

This work was supported by a National Research Foundation of Korea (NRF) grant funded by the Korean Government (MSIT) (RS-2024-00350440).

### References

- 1 J. P. Lee and T. Y. Ha: The Adequate Equity Estimation of Port SOC Investment. (Korea Maritime Institute, Busan, 2011) Chap. 3.
- 2 S. H. Lee and J. H. Lee: J. Korean GEO-environ. Soc. **12** (2011) 29. <https://doi.org/10.14481/jkges.2011.12.5.4>
- 3 S. H. Chun, S. I. Woo, C. K. Chung, and I. G. Choi: J. Korean Geotech. Soc. **23** (2007) 37. <https://doi.org/10.7843/kgs.2007.23.7.37>
- 4 K. W. Lee and B. D. Lee: KSCE J. Civ. Eng. **52** (2004) 36.
- 5 J. S. Jeon, K. H. Lee, and D. G. Yoon: J. Korean Geotech. Soc. **28** (2012) 39. <https://doi.org/10.7843/kgs.2012.28.6.39>
- 6 S. J. Kim: Korean J. Constr. Eng. Manag. **21** (2020) 45.
- 7 H. G. Kim and T. H. Roh: J. Korean Assoc. Geogr. Inf. Studies **17** (2014) 82. <http://dx.doi.org/10.11108/kagis.2014.17.3.082>
- 8 Y. W. Jang, Y. W. Choi, and G. S. Cho: KSCE J. Civ. Eng. **28** (2008) 269. <https://doi.org/10.12652/Ksce.2008.28.2D.269>
- 9 J. M. Kang, H. C. Yoon, K. S. Min, and G. J. We: Proc. Korean Soc. Surveying, Geodesy, Photogrammetry, and Cartography Conf. (Chuncheon, Korea, 2006) 533–540.
- 10 J. K. Park and K. Y. Jung: J. Korean Soc. Surv. Geodesy Photogramm. Cartogr. **38** (2020) 43. <https://doi.org/10.7848/ksgpc.2020.38.1.43>

- 11 J. H. Lee: Korea Maritime and Ocean Univ. (2023). <https://library.kmou.ac.kr/search/media/url/CAT000000367334>
- 12 S. H. Jung: Korea Univ. (2023). <https://www.doi.org/10.23186/korea.000000269787.11009.0001414>
- 13 J. S. Lee and J. H. Kwon: Proc. Korean Soc. Surveying, Geodesy, Photogrammetry, and Cartography Conf. (Seoul, Korea, 2019) 240–241.

